Journal of Biomedical Optics

BiomedicalOptics.SPIEDigitalLibrary.org

Photothermal ablation of liver tissue with 1940-nm thulium fiber laser: an *ex vivo* study on lamb liver

Heba Z. Alagha
Murat Gülsoy

SPIE.

Photothermal ablation of liver tissue with 1940-nm thulium fiber laser: an *ex vivo* study on lamb liver

Heba Z. Alagha and Murat Gülsoy*
Bogaziçi University, Biophotonics Laboratory, Institute of Biomedical Engineering, Kandilli Campus, ÇengelKöy, Istanbul 34684, Turkey

Abstract. The purpose of this study was to investigate the ablation efficiency of 1940-nm thulium fiber laser on liver tissue, while utilizing a real-time measurement system to monitor the temperature rise in adjacent tissues. Thulium fiber laser was delivered to lamb liver tissue samples via 400-μm bare tip fiber in contact mode. Eight different laser parameter combinations [power, continuous-wave (cw)/pulsed-modulated (pm) mode, and exposure time] were used. Exposure times were chosen to give the same total applied energy of 4 J for comparative purposes. Following laser irradiations, tissues were processed and stained with hematoxylin and eosin for macroscopic evaluation of ablation areas and total altered areas, and ablation efficiencies were calculated. Temperature of the nearby tissue at a distance of 1 mm from the fiber was measured, and rate of temperature change was calculated. A strong correlation between the rate of temperature change and ablation area was noted. Thermal effects increased with increasing power for both modes. The continuous-wave mode yielded higher ablation efficiencies than the pulse-modulated mode. Histological evaluation revealed a narrow vacuolization zone and negligible carbonization for higher-power values. [DOI: 10.1117/1.JBO.21.1.015007]

Keywords: ablation efficiency; liver surgery; rate of temperature change; thermal damage; thulium laser; 1940 nm.

Paper 150143RR received Apr. 2, 2015; accepted for publication Dec. 9, 2015; published online Jan. 20, 2016.

1 Introduction

Liver surgery is a general term encompassing different types of operations done on the liver for different diseases. The most common operation performed on the liver is a liver resection, which is the surgical removal of a portion of the liver. It is usually done to remove various types of liver tumors, both benign and malignant. However, this operation is limited to patients who have good liver function with one or two small (3 cm or less) tumors that have not grown into blood vessels.[1] The limited number of patients that can benefit from liver resection, in addition to the possible risks and side effects associated with conventional surgery like bleeding, blood clots, and infections, has motivated researchers to search for alternative therapies such as radio-frequency ablation, microwave ablation, cryotherapy, and laser therapy.

Radio-frequency ablation uses radio waves to destroy tumor cells with minimal morbidity, but it cannot be used if the tumor is big (over 3 cm) or is close to major blood vessels.[2] Microwave ablation is similar to radio-frequency ablation but uses microwaves. It is effective in treating fibrous tumors but cannot be used if the tumor is too close to another organ such as the bowel.[2,3] Cryotherapy uses extreme cold to destroy tumor cells. It can be used for treating metastatic tumors, but may cause damage to the bile ducts or major blood vessels, which may lead to hemorrhage.[3,4]

Lasers can be used to cut or coagulate tumor cells. As against conventional surgery, where cutting is done with the help of a sharp blade, laser can cut and coagulate at the same time, offering a bloodless operating field, no requirement for sutures, less operating time, minimal swelling and scars, and minimal postoperative pain.

Thermal effects of different lasers on soft tissues have been investigated in many scientific studies since the introduction of the Ruby laser in 1962.[5] As a result, many medical lasers have been developed for different therapeutic procedures. The wavelengths available for soft tissue surgery include CO_2, Nd:YAG, Er:YAG, Ho:YAG, diode lasers, and many others. The use of laser as a heat source to destroy liver tumors was first reported by Bown.[6] The treatment was referred to as laser-induced interstitial thermotherapy (LITT). LITT is gaining acceptance for the treatment of nonresectable liver tumors and as a potential alternative to surgery. The Nd:YAG laser (1064 nm) is currently the most commonly used laser system for LITT.[7–11] CO_2 (10,600 nm) and Er:YAG (2940 nm) lasers are good tissue ablation systems because their wavelengths are very close to water absorption peaks and thus they have a high rate of absorption by the "rich water content" soft tissues, giving them the ability to ablate precisely while providing good coagulation properties.[12–18] However, these wavelengths cannot be transmitted through silica fibers.

Thulium fiber lasers offer several advantages including smaller size, higher efficiency, improved spatial beam quality, operation in pulsed-modulated (pm) or continuous-wave (cw) mode, and inherent fiber optic beam delivery, which enables easy coupling to other fiber optics. The thulium fiber laser emitting at 1940 nm offers an additional advantage: this wavelength corresponds to one of the absorption peaks of water, which is the dominant absorber in tissue in the mid-infrared region, making it a potential tool for precise cutting and ablation of tissues.

The potential of thulium fiber lasers for hard and soft tissue surgery was investigated in the various studies.[19–23] Thulium fiber laser emitting at 1940 nm (the wavelength used for this study) was also investigated in a couple of studies for the vaporization of prostate,[24] partial kidney resection,[25] brain tissue ablation,[26] and intraoral surgery.[27] In these studies, thulium fiber

*Address all correspondence to: Murat Gülsoy, E-mail: gulsoy@boun.edu.tr

1083-3668/2016/$25.00 © 2016 SPIE

laser was shown to provide good ablation capabilities with sufficient hemostasis.

However, despite the advantages that lasers offer, the main drawback they have is the possible thermal damage to the surrounding tissues. An area of coagulation forms around the ablated area due to heat transport. This area can help in the sealing of the blood vessels.[18] However, it should be confined to prevent damage of healthy tissue. Fortunately, this can be achieved by the proper choice of laser wavelength and the proper adjustment of laser parameters. In addition to that, since temperature values reached within tissue and the spatial distribution of this temperature define the thermal effect and the amount of tissue undergoing thermal damage, respectively, monitoring temperature rise during laser irradiation of tissue can provide a useful feedback to adjust laser parameters to obtain the desired outcome with minimal thermal damage to surrounding healthy tissues.

The aim of this study was to investigate the ablation efficiency of different working modes and power settings of 1940-nm thulium fiber laser on liver tissue, while utilizing real-time measurement system to monitor temperature rise in adjacent tissues.

2 Materials and Methods

2.1 *Sample Collection and Preparation*

Fresh lamb livers purchased from a butcher were used for the experiments. Samples measuring $2 \times 4 \times 1$ cm^3 were cut, washed, and immersed in saline to prevent tissue dehydration. The samples were used within 12 h of animal sacrifice. Immediately before the experiments, the samples temperature was raised to room temperature between 21°C and 23°C. The temperature was measured using a K-type thermocouple. Four laser applications were done per sample. The applications were spaced 1 cm apart to allow enough space to avoid boundary effects. A total of 64 laser applications were performed in order to study eight different laser parameter combinations (power, mode, and exposure), with each parameter combination repeated eight times.

2.2 *Laser System and Laser Application Procedure*

Laser irradiations were performed using thulium fiber laser (TLR-5-1940; IPG Laser GmbH, Germany), which emits at 1940-nm wavelength, can work in continuous-wave mode and modulated (chopped) mode and has a maximum output power of 5 W. The term pulse-modulated mode was used to refer modulated mode. The laser parameters were controlled using the custom-built controller unit (Teknofil, Inc., Istanbul, Turkey) that could be accessed through a LabView interface. The output of the laser, which is provided through a 1-m fiber optic cable, was coupled to a flat-cut bare-ended optical fiber with a core diameter of 400 μm (NA $= 0.39 \pm 0.02$, low OH) by means of focusing lenses and xyz alignment apparatus. The fiber end was positioned perpendicular to the tissue surface in contact mode (0.5 mm inside the tissue). Before each laser application, the fiber distal end was checked for irregularities (in case of being broken or burned) and polished when necessary. The laser power at that end was also checked before each application using an optical power meter (PM 200; Thorlabs Inc., New Jersey) and thermal power sensor (S314C; Thorlabs Inc., New Jersey).

In order to determine the laser parameter combinations to be studied, a predosimetry study was conducted by exposing liver tissue samples to laser light and observing coagulation and carbonization onsets, and recording them for different power levels starting from 200 mW and increasing by small increments of 200 mW. When the power exceeded 800 mW, carbonization was observed consistently. Therefore, a range of powers (200 to 800 mW) that can be used safely (i.e., causing no carbonization) was set. The laser exposure times and pulse widths for both continuous-wave mode and pulse-modulated mode were chosen so that they deliver the same amount of laser energy (4 J) to the tissue, so that a convenient comparison between the different laser parameter combinations can be held. The laser parameter combinations used are listed in Table 1.

2.3 *Temperature Measurements*

Temperature of the nearby tissue was measured using a K-type thermocouple (KMTSS-010G-6; Omega) that can detect 0.1°C changes and has a response time of 0.1 s. The thermocouple tip was inserted at a distance of 0.5 mm inside the tissue (at the same level with the fiber tip) and placed 1 mm away from the optical fiber tip. The 1-mm distance was achieved using a special piece that was designed specifically for this purpose and manufactured using a three-dimensional printer. The piece had two holes that are 1 mm apart. The piece was mounted on a holder, and the fiber and the thermocouple were placed in the two holes. Temperature changes were observed real time via a LabView program that was run on a computer connected to the thermocouple controller.

2.4 *Histological Procedures*

Immediately after laser applications, rectangular blocks measuring 1 cm^3 containing the irradiated area surrounded by unaltered tissue were excised and fixed in a 10% formalin solution at 4°C for 66 ± 6 h. At the end of the fixation phase, the blocks were cut laterally at the laser irradiation sites and processed (dehydrated) using a tissue processing machine (Leica TP 1020; Leica Microsystems, Germany). Dehydrated tissues were then

Table 1 Laser parameter combinations applied to liver tissue.

Laser power (mW)	Laser mode	Duration (s)	Duty cycle (%)	Laser energy delivered (J)
200	cw	20	100	4
200	pm	40 (100 ms on, 100 ms off)	50	4
400	cw	10	100	4
400	pm	20 (100 ms on, 100 ms off)	50	4
600	cw	6.7	100	4
600	pm	13.4 (100 ms on, 100 ms off)	50	4
800	cw	5	100	4
800	pm	10 (100 ms on, 100 ms off)	50	4

Note: cw, continuous-wave mode and pm, pulse-modulated mode.

embedded in paraffin blocks using the paraffin embedding system (Leica EG1150, Leica Microsystems, Germany). We then obtained 10-μm sections using a microtome (RM 2255, Leica Microsystems, Germany) and aligned them on top of glass slides. Tissue sections were then stained with hematoxylin and eosin (H&E) to enable visualization of the thermal effects induced by laser irradiation on tissues under light microscopy.

2.5 *Ablation Efficiency and Thermal Damage Evaluation*

Tissue slides were visualized under light microscope (Eclipse 80i; Nikon Co., Tokyo, Japan), and images were captured at two magnifications, 4× and 10×. Imaging software (ImageJ; National Institute of Health) was used to measure ablated and total thermally altered areas. The total thermally altered area referred to irreversible thermal altered area (i.e., ablated and coagulated areas) excluding reversible thermal altered area as shown in Fig. 1. The histological discrimination criterion between irreversible thermal altered areas and reversible thermal altered areas was the absence and presence of nuclei in the stained tissue slides. Ablation efficiency was calculated according to the equation:

$$\text{Ablation efficiency} = \text{ablation area}/\text{total thermally altered area} \times 100\%$$

which was defined in the previous studies.[26–28]

2.6 *Data Analysis*

Means and standard deviations of ablation areas, total thermally altered areas, and temperature increases were calculated from eight independent samples for each set of the eight laser parameter combinations used. A two-way ANOVA was then conducted to reveal the effect of the two parameters (laser power and laser mode) on the ablation and total thermally altered areas as well as on the temperature increases. Tukey's test was then used as a *post hoc* test to determine the statistical differences between the ablated and total thermally altered areas and temperature increases with respect to the two parameters (laser power and laser mode). The significant level was set to $P < 0.05$. The term "rate of temperature change" was defined as the maximum temperature increase divided by the time to reach that maximum, then Pearson's correlation coefficient was used to reveal the relationship between this rate of temperature change and ablated and total thermally altered areas.

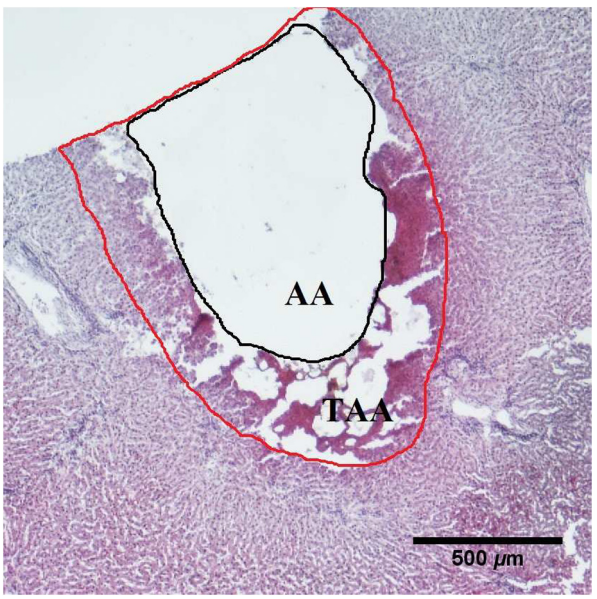

Fig. 1 Liver tissue exposed to 1940-nm thulium fiber laser at 800 mW and continuous-wave mode for a duration of 5 s (4× magnification). AA, ablated area and TAA, total altered area.

3 Results

This research focused mainly on investigating the effect of different power and mode settings of 1940-nm thulium fiber laser on ablation areas, total thermal damage areas, and temperature changes when applied to liver tissue.

A two-way ANOVA revealed that the two parameters (laser power and laser mode) had a significant effect on ablation area and total altered area ($P < 0.001$). Regarding ablation efficiency, the effect of laser mode was significant, but the effect of laser power was not.

3.1 *Ablation Area, Total Altered Area, and Ablation Efficiency*

The mean values of ablation areas, total altered areas, and ablation efficiencies are plotted in Fig. 2. The biggest ablation area and total altered area were achieved at 800 mW of continuous-wave mode, while the highest ablation efficiency of 75% was achieved at 400 mW of continuous-wave mode.

For continuous-wave mode, there was a significant difference in ablation area for the different power settings (200, 400, 600, and 800 mW). Increasing the power resulted in higher ablation areas ($P < 0.001$). Total altered area also increased with increasing the power. Tukey's test showed that there was a significant difference in total altered area between the different power groups ($P < 0.005$) except between the power settings of 200 and 400 mW where there was no significant difference ($P > 0.05$). Regarding ablation efficiency, 200 mW resulted in significantly smaller ablation efficiency when compared to 400, 600, and 800 mW ($P < 0.05$). However, power settings 400, 600, and 800 mW resulted in almost the same ablation efficiencies ($P > 0.05$).

For pulse-modulated mode, increasing the power resulted in significantly higher ablation areas and total altered areas ($P < 0.05$). However, the effect of laser power on ablation efficiency was not significant. Regardless of the power values, ablation efficiency was almost the same.

Changing the mode of laser while keeping the power constant resulted in significantly different values in ablation area, total altered area, and ablation efficiency for all power values used. continuous-wave mode produced higher ablation areas, total altered areas, and ablation efficiencies. The only exception was at 200 mW where there was no significant difference in ablation efficiency between continuous-wave mode and pulse-modulated mode.

3.2 *Temperature Measurements*

Temperature of the nearby tissue was measured at a distance of 1 mm. For each sample, the maximum temperature increase with respect to prelaser temperature (mean = 21°C) ΔT, the time duration to reach that maximum, and the rate of temperature change (calculated as the maximum temperature increase ΔT

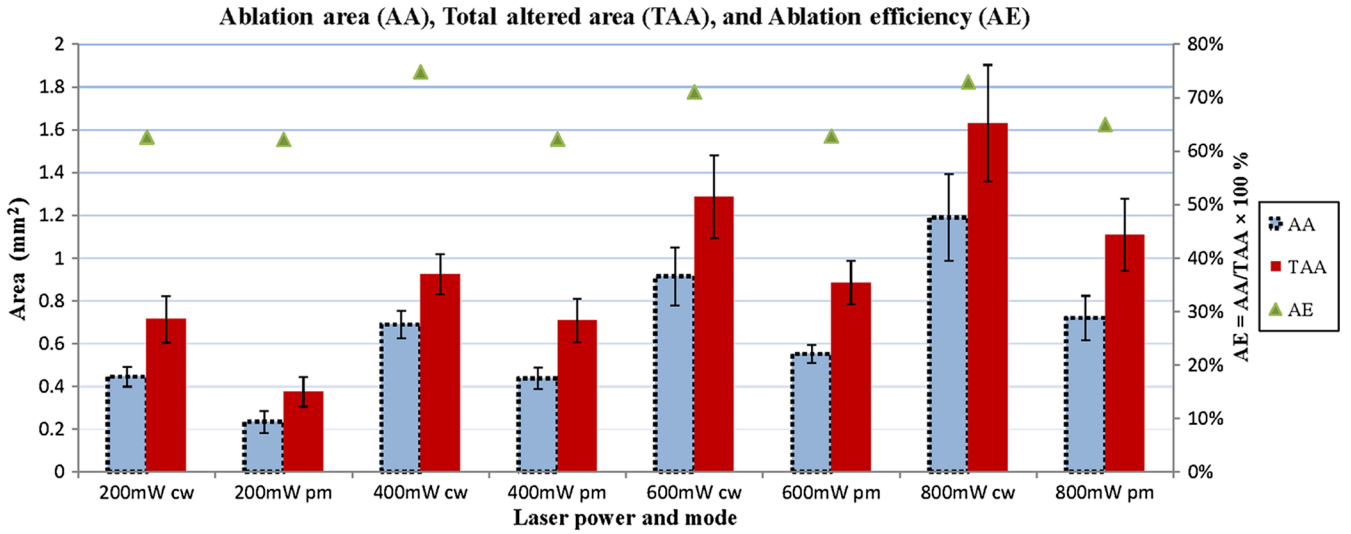

Fig. 2 Mean ablation areas, total altered areas, and ablation efficiencies for the eight different laser parameter combinations studied. The values are the mean values of eight experiments. AA, ablated area; TAA, total altered area; AE, ablation efficiency; cw, continuous-wave mode; and pm, pulse-modulated mode.

divided by the time duration to reach that temperature) were calculated. Table 2 shows mean values of these variables (obtained from eight independent samples).

For both continuous-wave and pulse-modulated modes, increasing the power resulted in higher temperatures. For the same power, continuous-wave mode resulted in higher temperatures compared to pulse-modulated mode.

The rate of temperature change was slowest at 200 mW of pulse-modulated mode (0.13 ± 0.01°C/s) and fastest at 800 mW of continuous-wave mode (3.58 ± 0.47°C/s). A two-way ANOVA revealed that the rate of temperature change was differentiated by the two parameters laser power ($P < 0.001$) and laser mode ($P < 0.001$). For both continuous-wave and pulse-modulated modes, increasing the power resulted in higher rates of temperature change. For the same power, continuous-wave mode resulted in higher rates of temperature change compared to pulse-modulated mode.

Table 2 Temperature change and rate of temperature change for the eight laser parameter combinations studied.

Laser power (mW)	Laser mode	Temperature increase ΔT (°C)	Time (s)	ΔT/Time (°C/s)
200	cw	8.12 ± 0.87	20.08 ± 0.42	0.40 ± 0.04
200	pm	5.24 ± 0.36	38.96 ± 0.90	0.13 ± 0.01
400	cw	11.14 ± 2.20	10.50 ± 1.11	1.10 ± 0.37
400	pm	7.08 ± 0.26	20.16 ± 0.39	0.35 ± 0.02
600	cw	14.75 ± 1.14	7.05 ± 0.29	2.10 ± 0.21
600	pm	10.42 ± 1.82	13.53 ± 0.24	0.77 ± 0.13
800	cw	18.82 ± 2.20	5.28 ± 0.27	3.58 ± 0.47
800	pm	11.95 ± 1.32	10.10 ± 0.33	1.19 ± 0.16

Note: All values are shown as mean value ± standard deviation. Values are the means of eight experiments. ΔT, maximum temperature change with respect to the prelaser temperature (in °C); Time, time to reach maximum temperature from the start of laser irradiation (in s); ΔT/Time, rate of temperature increase (in °C s^{-1}); cw, continuous-wave mode; and pm, pulse-modulated mode.

Pearson's correlation coefficient revealed a strong correlation between the rate of temperature change and the ablation area for both continuous-wave mode ($R = 0.89$) and pulse-modulated mode ($P = 0.90$). Regardless of the laser delivery mode, the higher the rate of change of temperature is, the higher the ablation area.

A graph of the mean temperature values measured during and after laser irradiation was plotted over time for the different powers and modes used. Figure 3 shows the results obtained for the eight different laser parameter combinations together. In all applications, laser was applied at time $t = 5$ s.

The figure shows that the temperature increase was exponential. To better describe the temperature increase, an exponential equation was fitted to the data up to the maximum temperature in each curve. Values of the exponents were 0.016, 0.005, 0.045, 0.015, 0.080, 0.030, 0.135, and 0.049 s^{-1} for the groups 200 mW cw, 200 mW pm, 400 mW cw, 400 mW pm, 600 mW cw, 600 mW pm, 800 mW cw, and 800 mW pm, respectively. For both continuous wave and pulse-modulated modes, the exponents increased rapidly as the power values increased which was reflected as steeper slopes of the curves of higher power values as seen in Fig. 3. For the same power value, higher exponent values were correlated with continuous wave mode than pulse-modulated mode which resulted in steeper slopes of curves of continuous wave mode when compared to curves of pulse-modulated mode.

An exponential decay equation was fitted to the data obtained after the laser was switched off, from the maximum temperature until the final temperature, in each curve. Values of the exponents were −0.003, −0.003, −0.004, −0.003, −0.005, −0.005, −0.007, −0.006 s^{-1} for the groups 200 mW cw, 200 mW pm, 400 mW cw, 400 mW pm, 600 mW cw, 600 mW pm, 800 mW cw, and 800 mW pm, respectively. It can be seen from the figure, and from the values of the exponents, that the tissue took a relatively long time to cool down to its prelaser temperature

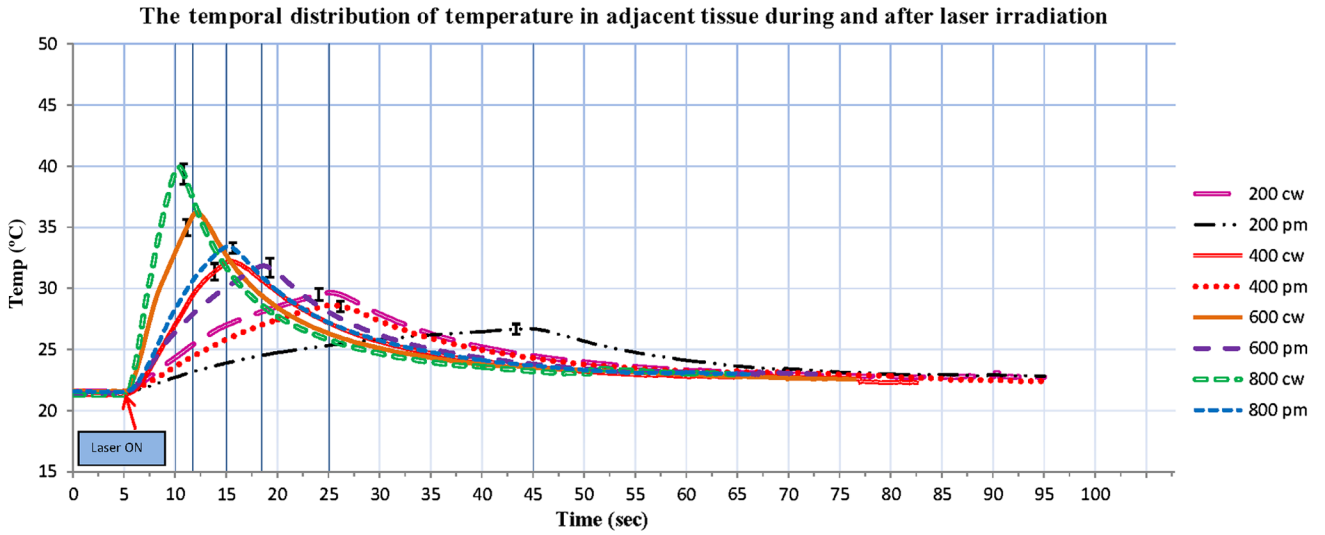

Fig. 3 The temporal distribution of temperature in adjacent tissues during and after laser irradiation. The laser was switched on at time $t = 5$ s. Vertical lines show the times the laser was switched off ($t = 10$ s for 800 mW cw, $t = 11.7$ s for 600 mW cw, $t = 15$ s for 800 mW pm and 400 mW cw, $t = 18.4$ s for 600 mW pm, $t = 25$ s for 400 mW pm and 200 mW cw, and $t = 45$ s for 200 mW pm).

compared to the time it took to reach the maximum temperature regardless of the laser delivery mode and power. Differences in the decay exponents were small and that was expected as temperature decay is a tissue-specific value.

The fact that the temperature increase was exponential led us to think that calculating the rate of temperature change along the total time to reach the maximum temperature might not make real sense. So, a comparison of the rate of temperature change within the first 2 s (after laser was switched on), where the temperature increase was estimated to be linear, was held (results not shown). Fortunately similar results were obtained; for both continuous-wave and pulse-modulated modes, increasing the power resulted in higher rates of temperature change. For the same power, continuous-wave mode resulted in higher rates of temperature change compared to pulse-modulated mode.

It can also be seen from Fig. 3 that temperature rises were quite similar for curves with same average power, e.g., 400 mW of continuous-wave mode and 800 mW of pulse-modulated mode (average power of 400 mW), and 200 mW of continuous-wave mode and 400 mW of pulse-modulated mode (average power of 200 mW). Exponent values of the temperature increase for 400 mW cw and 800 mW pm were 0.045 and 0.049 s^{-1}, respectively, while exponent values of the temperature increase for 200 mW cw and 400 mW pm were 0.016 and 0.015 s^{-1}, respectively. A two-way ANOVA revealed that there was no significant difference in temperature rise between 400 mW of continuous-wave mode and 800 mW of pulse-modulated mode. However, for the 200 mW of continuous-wave mode and 400 mW of pulse-modulated mode, a two-way ANOVA revealed that there was a significant difference in temperature rise between the two groups.

3.3 *Histological Evaluation*

Figure 4 shows an example of the H&E-stained lateral section induced by 200 mW of continuous-wave mode for a duration of 20 s. The slice shows the thermal effects of laser radiation as indexed: "1" ablated area, "2" coagulated area, "3" heat-affected area, and "4" normal tissue. No signs of carbonization were visible in this slice.

Histological evaluation of the H&E-stained lateral sections induced by the eight laser parameter combinations used revealed that ablation depth tended to increase with increasing power more than ablation width, but the overall result was a larger ablation area. Coagulation area also increased with increasing power. Some vacuolization was seen in the coagulated area. Carbonization was rarely seen. It was only seen for some of the 800 mW samples in a small amount. An area of heat-affected tissue that appeared as lighter tissue was visible in most of the samples. This area was considered as a reversible damage area since nuclei were clearly visible on it, and was not included in calculations of the total altered area that was calculated as ablation area plus coagulation area only, i.e., irreversible damage area.

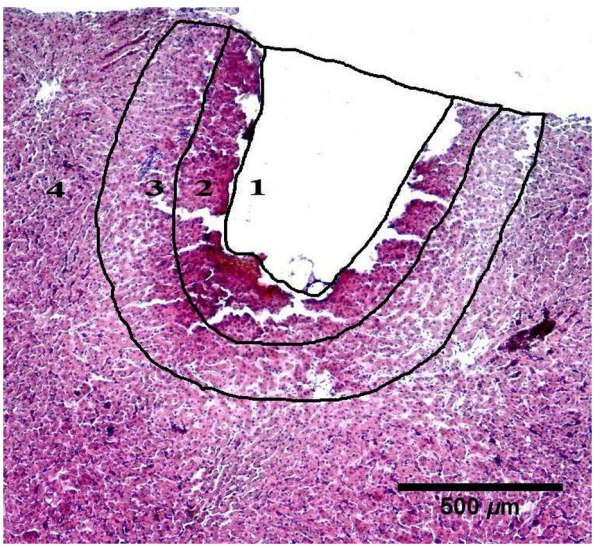

Fig. 4 Lateral section of H&E-stained liver tissue induced by 200 mW of cw mode at 20 s (magnification 4×). 1, ablated area (AA); 2, coagulated area; 3, heat-affected area; and 4, normal tissue. Areas 1 and 2 constitute the TAA.

4 Discussion

Lasers of wavelengths around 2 μm are strongly absorbed by water, the main constituent of all biological tissues. Absorption of these wavelengths by a volume of tissue results in a direct and immediate heating of the tissue. This allows for a very precise cutting of the tissue. Furthermore, the bleeding during the cutting is repressed by coagulation. This endows the 2-μm lasers with a high application potential in surgery and therapy.

The relatively new thulium fiber laser emitting at 1940 nm, which coincides with one of the absorption peaks of water, was investigated in a couple of studies for the ablation of soft and hard urinary stones,[29] the vaporization of prostate,[24] and the resection of kidney.[25] Our laboratory investigated it for brain surgery[26] and intraoral surgery.[27] In this study, we proposed the use of thulium fiber laser as an ablative tool for liver surgery. To investigate its efficacy on liver tissue, the ability of the laser to ablate and cut precisely was not our only concern. Minimizing thermal damage to surrounding tissue was as important as well. In order to achieve this, a detailed dosimetry study was carried out to determine the optimal parameters that would lead to the best ablation efficiency with minimal thermal damage. In addition to that, a temperature measurement system was used to monitor temperature increase in adjacent tissue. Temperature is certainly the governing parameter in photothermal interactions; the temperature values reached within tissue and the temporal duration of these temperatures define the thermal damage, and the spatial distribution of these temperatures define the amount of tissue undergoing thermal damage. Therefore, monitoring temperature increase during laser irradiation of tissue provides a useful feedback to adjust the laser parameters to obtain the desired outcome with minimal thermal damage to surrounding healthy tissue.

4.1 *Laser Power*

Ablation area and total altered area both increased with increasing power for both continuous-wave mode and pulse-modulated mode. This is consistent with the previous studies.[26,27,30,31] It was observed that the increase in ablation depth with increasing power was more than the increase in ablation width. This suggests that the ablation velocity in the depth (in the direction of laser irradiation) is faster than the temperature diffusion which remains about constant. This can be a result of using a flat-cut optical fiber. A diffusing fiber, e.g., could have resulted in a more circular shape of the ablation crater. The coagulation in both radial and lateral directions showed comparable sizes (probably due to temperature diffusion which remains about constant), which suggest that a precise defined coagulation in both directions could be achieved and this can be of interest with regard to sealing blood vessels around ablation area during *in vivo* situations; however, this suggestion should be verified in further *ex vivo* and *in vivo* experiments.

The increase in both ablation area and total altered area resulted in similar ablation efficiency (defined as the ratio of ablation area to total altered area) for all power groups in both continuous-wave and pulse-modulated modes. Only the 200 mW of continuous-wave mode group yielded significantly lower ablation efficiency than the other power groups in the continuous-wave mode, while in the pulse-modulated mode, there was no significant difference in all power groups. Perry et al.[32] reported a similar situation for Nd:YAG laser on oral tissue. They reported that cutting efficiency was not significantly improved by increasing power.

It can be noticed from Fig. 2 that 200 mW of continuous-wave mode and 400 mW of pulse-modulated mode resulted in similar thermal effects. In fact, the two groups have the same time duration of 20 s and thus the same average power of 200 mW. A two-way ANOVA revealed that there was no significant difference in ablation area, total altered area, and ablation efficiency between the two groups. For 400 mW of pulse-modulated mode and 800 mW of continuous-wave mode which both have a time duration of 10 s and thus the same average power of 400 mW, a two-way ANOVA revealed that there was no significant difference in the ablation area between the two groups; however, the difference in total altered area and ablation efficiency was significant ($P < 0.02$). The fact that same average power resulted in similar ablation area suggests that not only the peak power but also the average power should be taken into account when adjusting laser parameters for a given surgical procedure.

With a maximum of 75% and a minimum of 62%, all ablation efficiencies achieved were above 50% and were specified as successful.[18] Ablation efficiencies above 70% can be even specified as highly efficient. The high ablation efficiencies achieved coupled with the fact that the ablation efficiency was independent of the power value used can be of great interest because it implies that regardless of the power value used, high level of ablation will be achieved. Therefore, according to the specifications and desired outcomes of the laser intervention such as the size of the area to be ablated, the maximum duration of laser application, and the width of coagulation required, the power can be set and a successful ablation can be achieved.

4.2 *Mode of Operation*

It was observed that both ablation area and total altered area increased when changing the mode from pulse-modulated mode to continuous-wave mode while keeping the power constant, for all the four power values used in our experiment. However, the increase in ablation area was sharper and this caused the ablation efficiency to increase significantly between the two modes except at 200 mW where the difference was shown to be not significant. Continuous-wave mode was shown to yield a higher ablation than pulsed mode in the previous published data.[26] This can be explained by the fact that in continuous-wave mode, the continuous exposure to laser radiation causes the tissue to heat up rapidly resulting in tissue temperatures that can exceed vaporization threshold. Therefore, tissue water is removed quickly, and ablation of tissues dominates; more laser energy is consumed in ablation process than in heating nearby tissues, which results in higher ablation efficiencies. In pulse-modulated mode, the tissue is heated at a slower rate, and during the OFF period, there is time for the tissue to cool itself and conduct the heat to nearby tissue, so there is a decrease in the laser energy consumed in ablation process, resulting in lower ablation areas, which in turn results in lower ablation efficiencies.

4.3 *Temperature Increase*

During laser irradiation, temperature of the nearby tissue was measured at a distance of 1 mm using a K-type thermocouple with a response time of 0.1 s. The measurement was kept after the laser was turned off and continued until the normal temperature was reached again. The recorded measurements provided

us with the maximum temperatures reached, the time durations to reach these temperatures, as well as the time durations for the tissue to cool down. The rate of temperature change was calculated as the maximum temperature increase divided by the time duration to reach that temperature. Our results revealed that there was a strong correlation between rate of temperature change and ablation area. A fast and sudden increase in temperature resulted in higher ablation areas, with the highest rate of temperature change of $3.58 \pm 0.47°C/s$ corresponding to the highest ablation area of 1.19 ± 0.20 mm^2 achieved at 800 mW of continuous-wave mode, whereas a slow and prolonged rate of increase in temperature resulted in lower ablation areas, with the slowest rate of $0.13 \pm 0.01°C/s$ corresponding to the lowest ablation area of 0.23 ± 0.05 mm^2 achieved at 200 mW of pulse-modulated mode.

A strong correlation was also revealed between rate of temperature change and total altered area. Higher total altered areas also corresponded to higher rates of temperature change and vice versa. This dual correlation between both ablation area and total altered area with rate of temperature change resulted in a weak correlation between rate of temperature change and ablation efficiency for both continuous-wave mode ($R = 0.43$) and pulse-modulated mode ($R = 0.27$).

The high correlation between the rate of temperature change and ablation and total altered areas can be of interest as it means that the temperature of adjacent tissue can be used as a real-time reference that a laser applicator can use to predict the ablation and coagulation areas and estimate the thermal damage, and use this information to adjust the laser parameters to minimize the collateral thermal damage to adjacent tissues.

Higher powers and continuous-wave mode yielded higher temperature peaks, and rates of temperature change than lower powers and pulse-modulated mode, which is consistent with the previous studies.[26,32,33]

Referring back to Table 2, the range of temperature increase was from 5.24°C to 18.82°C. These values should be considered in light of the measurement system and the fact that they were measurements of nearby tissue measured at a distance of 1 mm from the laser application site. There are two aspects that tend to have opposite effects on the measurements: one tends to overestimate the results and the second tends to underestimate the results. The first aspect is related to the metallic constitution of the thermocouple. The metal conductors of the thermocouple absorb laser radiation and cause a local and instantaneous increase in temperature, which entails an overestimation of the actual temperatures measured. Solution to this artifact was suggested in different studies.[34–37] In our study, the thermocouple was inserted at a distance of 1 mm from the laser fiber. Within this distance, the intensity of the laser light was reduced to an amount that would have a negligible effect on the thermocouple. The presence of a sudden increase or decrease in temperature when the laser was turned on and off was not visible (Fig. 3).

The second aspect is the time response of the temperature measurement system. In our study, it was 0.1 s, which is much slower than the thermal response of the tissue to laser irradiation, which is at the nanosecond level as reported previously.[38] Hence, for more accurate estimation of the real tissue temperature, a measurement system with a faster response time is suggested to be used.

It was noticed also that the time to reach the maximum temperature was sometimes longer than the irradiation time. This can be attributed to thermal conductivity of liver tissue; the thermal pulse dissipated within the tissue takes some time to reach the thermocouple tip placed at a distance of 1 mm from the irradiation site (the max temperature position). Since thermal conductivity is tissue specific, one can benefit from this time delay in estimating the thermal conductivity of the tissue.

The high variability of temperature increase as shown in Table 2 could be due to the fact that an exact 1-mm distance was difficult to achieve and not always possible due to the very soft and delicate nature of liver tissue. Another reason could be due to tissue inhomogeneity.

The temperature of nearby tissues can be a good real-time reference for the laser applicator to estimate the thermal damage of tissues. However, this can be improved using more than one thermocouple on different sides of the targeted tissue, as well as on different depths to monitor the temperature on every direction and depth to give a more precise image on what is going on.

The results obtained in this experiment should be considered in light of the limitations of *ex vivo* studies despite the steps that were taken to simulate *in vivo* conditions such as the use of fresh samples and immersion in saline. Loss of perfusion in *ex vivo* studies means loss of chromophores that may influence performance of the laser. Blood perfusion can provide a cooling effect under *in vivo* conditions that could affect the thermal response of the tissue to the applied laser radiation. Smaller ablation areas and less temperature increases are expected compared to *ex vivo*.

This study was performed on normal liver tissue only. The difference in thermal and optical properties between normal and tumor tissues may influence the mechanisms by which tissue is heated, and therefore, the effect of thulium fiber laser on tumor liver tissue may vary.[39,40] Further experiments should be carried out to investigate the effect of thulium fiber laser on tumor liver tissue.

Future work should also taken into account the continuous changes in the optical properties of tissues (and thus, the change in the absorption coefficient of water) that result as the tissue is being heated following absorption of laser light.[41,42] These dynamic changes affect the tissue response to laser radiation[43] and can sometimes reduce the effectiveness of even the best dose estimate. So, the application parameters should not be kept constant but should be adjusted continuously to provide the desired outcome with minimal thermal damage to surrounding tissue.

5 Conclusion

The aim of this study was to investigate the thermal effects of 1940-nm thulium fiber laser on liver tissues and to monitor temperature rise in adjacent tissues. The study showed that the temperature of nearby tissue can be used as real-time reference by the laser applicator to estimate the thermal effects and accordingly avoid thermal damage to adjacent tissues. 1940-nm thulium fiber laser was shown to ablate and coagulate with a good efficiency. Further *in vivo* studies should be carried out to investigate the ablation capabilities of 1940-nm thulium fiber laser on liver tumor tissue and to evaluate the exact coagulation and hemostasis properties; to verify if a precise defined coagulation in both radial and lateral directions is achieved, and to show whether the coagulation induced can seal small and large blood vessels alike.

Acknowledgments

This work was supported by the Bogazici University Research Fund (Project no: BAP 6649–12XM3) and partly by TUBITAK Research Project 107E119.

References

1. T. L. Fong, "Liver resection," 8 June 2015, http://www.medicinenet.com/liver_resection/article.htm (9 March 2015).
2. "Types of treatments for liver cancer," 28 February 2015, http://www.cancerresearchuk.org/about-cancer/type/liver-cancer/treatment/which-treatment-for-liver-cancer (1 September 2015).
3. G. D. Dodd et al., "Minimally invasive treatment of malignant hepatic tumors: at the threshold of a major breakthrough," *Radiographics* **20**(1), 9–27 (2000).
4. "Cryosurgery in cancer treatment: questions and answers," 10 September 2015, http://www.cancer.gov/about-cancer/treatment/types/surgery/cryosurgery-fact-sheet (14 September 2015).
5. C. H. Townes, *How the Laser Happened: Adventures of a Scientist*, Oxford University Press, Inc., New York (1999).
6. S. G. M. Bown, "Phototherapy of tumors," *World J. Surg.* **7**(6), 700–709 (1983).
7. M. Nikfarjam and C. Christophi, "Interstitial laser thermotherapy for liver tumors," *Br. J. Surg.* **90**(9), 1033–1047 (2003).
8. E. Rohde et al., "Interstitial laser-induced thermotherapy (LITT): comparison of in-vitro irradiation effects of Nd:YAG (1064 nm) and diode (940 nm) laser," *Med. Laser Appl.* **16**(2), 81–90 (2001).
9. F. A. Jolesz and G. P. Zientara, "MRI-guided laser-induced interstitial thermotherapy: basic principles," in *Laser-Induced Interstitial Thermotherapy*, G. J. Müller and A. Roggan, Eds., pp. 294–324, SPIE Optical Engineering Press, Bellingham, Washington (1995).
10. A. Masters et al., "Interstitial laser hyperthermia: a new approach for treating liver metastases," *Br. J. Cancer* **66**(3), 518 (1992).
11. R. Muschter et al., "Clinical results of LITT in the treatment of benign prostatic hyperplasia: comparison of Nd:YAG and diode laser," in *Laser-Induced Interstitial Thermotherapy*, G. J. Müller and A. Roggan, Eds., pp. 434–442, SPIE Optical Engineering Press, Bellingham, Washington (1995).
12. R. M. Pick and B. C. Pecaro, "Use of the CO_2 laser in soft tissue dental surgery," *Lasers Surg. Med.* **7**(2), 207–213 (1987).
13. S. Barak and I. Kaplan, "The CO_2 laser in the excision of gingival hyperplasia caused by nifedipine," *J. Clin. Periodontol.* **15**, 633–635 (1988).
14. L. J. Christenson, K. Smith, and C. Arpey, "Treatment of multiple cutaneous leiomyomas with CO_2 laser ablation," *Dermatologic Surg.* **26**, 319–322 (2000).
15. U. Hohenleutner et al., "Fast and effective skin ablation with an Er:YAG laser: determination of ablation rates and thermal damage zones," *Lasers Surg. Med.* **21**(3), 242–247 (1997).
16. B. Drnov šek-Olup and B. Vedlin, "Use of Er:YAG laser for benign skin disorders," *Lasers Surg. Med.* **21**(1), 13–19 (1997).
17. G. Teikemeier and D. J. Goldberg, "Skin resurfacing with the erbium: YAG laser," *Dermatologic Surg.* **23**(8), 685–687 (1997).
18. M. H. Niemz, *Laser–Tissue Interactions: Fundamentals and Applications*, Springer, New York (2007).
19. R. L. Blackmon, P. B. Irby, and N. M. Fried, "Comparison of holmium:YAG and thulium fiber laser lithotripsy: ablation thresholds, ablation rates, and retropulsion effects," *J. Biomed. Opt.* **16**(7), 071403 (2011).
20. A. K. Ngo et al., "Laser welding of urinary tissues, ex vivo, using a tubable Thulium fiber laser," *Proc. SPIE* **6078**, 60781B (2006).
21. R. S. Blokker, T. M. T. W. Lock, and T. de Boorder, "Comparing thulium laser and Nd:YAG laser in the treatment of genital and urethral condylomata acuminate in male patients," *Lasers Surg. Med.* **45**(9), 582–588 (2013).
22. S. J. Xia et al., "Thulium laser resection of prostate-tangerine technique in treatment of benign prostate hyperplasia," *Zhonghua Yi Xue Za Zhi* **85**(45), 3225–3228 (2005).
23. S. J. Xia et al., "Thulium laser versus standard transurethral resection of the prostate: a randomized prospective trial," *Eur. Urol.* **53**(2), 382–390 (2008).
24. N. M. Fried and K. E. Murray, "High-power thulium fiber laser ablation of urinary tissues at 1.94 μm," *J. Endourol.* **19**(1), 25–31 (2005).
25. D. Theisen-Kunde et al., "Partial kidney resection based on 1.94 μm fiber laser system," *Proc. SPIE* **6632**, 663205 (2007).
26. B. Tunc and M. Gulsoy, "Tm: fiber laser ablation with real-time temperature monitoring for minimizing collateral thermal damage: ex vivo dosimetry for ovine brain," *Lasers Surg. Med.* **45**(1), 48–56 (2013).
27. M. Guney, B. Tunc, and M. Gulsoy, "Investigating the ablation efficiency of a 1940-nm thulium fiber laser for intraoral surgery," *Int. J. Oral Maxillofac. Surg.* **43**(8), 1015–1021 (2014).
28. T. Bilici et al., "Development of thulium (Tm:YAP) laser system for brain tissue ablation," *Lasers Med. Sci.* **26**(5), 699–706 (2011).
29. N. M. Fried, "Thulium fiber laser lithotripsy: an in vitro analysis of stone fragmentation using a modulated 110-W thulium fiber laser at 1.94 μm," *Lasers Surg. Med.* **37**, 53–58 (2005).
30. E. Merigo et al., "Laser-assisted surgery with different wavelengths: a preliminary ex vivo study on thermal increase and histological evaluation," *Lasers Med. Sci.* **28**(2), 497–504 (2013).
31. J. I. Youn and J. D. Holcomb, "Ablation efficiency and relative thermal confinement measurements using wavelengths 1,064, 1,320, and 1,444 nm for laser-assisted lipolysis," *Lasers Med. Sci.* **28**(2), 519–527 (2013).
32. D. A. Perry, H. E. Goodis, and J. M. White, "In vitro study of the effects of Nd:YAG laser probe parameters on bovine oral soft tissue excision," *Lasers Surg. Med.* **21**(1), 39–46 (1997).
33. W. S. J. Malskat et al., "Temperature profiles of 980-and 1,470-nm endovenous laser ablation, endovenous radio frequency ablation and endovenous steam ablation," *Lasers Med. Sci.* **29**(2), 423–429 (2014).
34. P. Saccomandi, E. Schena, and S. Silvestri, "Techniques for temperature monitoring during laser-induced thermotherapy: an overview," *Int. J. Hyperthermia* **29**(7), 609–619 (2013).
35. B. Anvari et al., "Effects of surface irrigation on the thermal response of tissue during laser irradiation," *Lasers Surg. Med.* **14**(4), 386–395 (1994).
36. F. Manns et al., "In situ temperature measurements with thermocouple probes during laser interstitial thermotherapy (LITT): quantification and correction of a measurement artifact," *Lasers Surg. Med.* **23**(2), 94–103 (1998).
37. S. A. Van Nimwegen et al., "Nd:YAG surgical laser effects in canine prostate tissue: temperature and damage distribution," *Phys. Med. Biol.* **54**(1), 29 (2009).
38. M. Ishihara et al., "Measurement of the surface temperature of the cornea during ARF excimer laser ablation by thermal radiometry with a 15-nanosecond time response," *Lasers Surg. Med.* **30**(1), 54–59 (2002).
39. R. van Hillegersberg et al., "Optical properties of rat liver and tumor at 633 nm and 1064 nm: photofrin enhances scattering," *Lasers Surg. Med.* **13**(1), 31–39 (1993).
40. C. T. Germer et al., "Optical properties of native and coagulated human liver tissue and liver metastases in the near infrared range," *Lasers Surg. Med.* **23**(4), 194–203 (1998).
41. E. D. Jansen et al., "Temperature dependence of the absorption coefficient of water for midinfrared laser radiation," *Lasers Surg. Med.* **14**(3), 258–268 (1994).
42. B. I. Lange, T. Brendel, and G. Hüttmann, "Temperature dependence of light absorption in water at holmium and thulium laser wavelengths," *Appl. Opt.* **41**(27), 5797–5803 (2002).
43. J. T. Walsh and J. P. Cummings, "Effect of the dynamic optical properties of water on midinfrared laser ablation," *Lasers Surg. Med.* **15**(3), 295–305 (1994).

Heba Z. Alagha is a PhD student at the Institute of Biomedical Engineering at Boğaziçi University where she received her MS degree in biomedical engineering. She did her BS in computer engineering from the University of Jordan. Her current research interests include laser-tissue interactions, photothermal applications of lasers, and photodynamic therapy. She is a member of SPIE.

Murat Gülsoy is a professor at the Institute of Biomedical Engineering at Boğaziçi University where he received his BS degree in electrical engineering and MA degree in psychology. He did his PhD in biomedical engineering from Istanbul Technical University where he studied thermal aspects of laser–tissue interactions. His current research interests include laser–tissue interactions, biostimulation, surgical laser systems, photodynamic therapy, lasers in dentistry, measurement of optical properties, laser tissue welding, and photothermal applications. He is a member of SPIE.